



HAL
open science

Simple carrier-envelope phase control and stabilization scheme for difference frequency generation-based systems

Michele Natile, Florent Guichard, Yoann Zaouter, Marc Hanna, Patrick Georges

► To cite this version:

Michele Natile, Florent Guichard, Yoann Zaouter, Marc Hanna, Patrick Georges. Simple carrier-envelope phase control and stabilization scheme for difference frequency generation-based systems. *Optics Express*, 2021, 29 (11), pp.16261-16269. 10.1364/oe.424141 . hal-03251566

HAL Id: hal-03251566

<https://hal-iogs.archives-ouvertes.fr/hal-03251566>

Submitted on 7 Jun 2021

HAL is a multi-disciplinary open access archive for the deposit and dissemination of scientific research documents, whether they are published or not. The documents may come from teaching and research institutions in France or abroad, or from public or private research centers.

L'archive ouverte pluridisciplinaire **HAL**, est destinée au dépôt et à la diffusion de documents scientifiques de niveau recherche, publiés ou non, émanant des établissements d'enseignement et de recherche français ou étrangers, des laboratoires publics ou privés.



Simple carrier-envelope phase control and stabilization scheme for difference frequency generation-based systems

MICHELE NATILE,^{1,*} FLORENT GUICHARD,¹ YOANN ZAOUTER,¹
MARC HANNA,²  AND PATRICK GEORGES²

¹*Amplitude, 11, Avenue de la Canteranne, 33600 Pessac, France*

²*Université Paris-Saclay, Institut d'Optique Graduate School, CNRS, Laboratoire Charles Fabry, 91127 Palaiseau, France*

**michele.natile@amplitude-laser.com*

Abstract: We report about a setup for carrier-envelope phase (CEP) control and stabilization in passive systems based on difference frequency generation (DFG). The principle of this approach relies on the amplitude to phase modulation transfer in the white-light generation process. A small modulation of the pump laser intensity is used to obtain a DFG output modulated in CEP. This technique is demonstrated in a CEP-stable system pumped by an Yb-doped fiber amplifier. It is first characterized by measuring CEP modulations produced by applying arbitrary waveforms. The CEP actuator is then used for slow drifts correction in a feedback loop. The results show the capability of this simple approach for OPA/OPCPA CEP-stabilized setups.

© 2021 Optical Society of America under the terms of the [OSA Open Access Publishing Agreement](#)

1. Introduction

Carrier-envelope phase (CEP) stabilization is an essential feature allowing access to complete control over the electric field generated by femtosecond lasers. This control opens a wide range of applications going from frequency combs applications [1], such as spectroscopy [2], to strong-field physics using few-cycle pulses [3,4]. A CEP-stable femtosecond laser source is, indeed, required to obtain isolated attosecond pulses via the high-harmonic generation phenomenon [5].

Several approaches have been proposed for the stabilization and control of the CEP of oscillators [6,7] and amplifiers [8]. These approaches can be divided into active and passive stabilization whether an electronic feedback loop is used or not to lock the CEP.

Active stabilization has been used both for oscillators and amplifiers stabilization setups. For oscillators, the carrier envelope offset frequency (f_{CEO}) is detected at the oscillator output and a feedback loop acting on a CEP active element inside or outside the cavity achieves the stabilization [9]. A commonly and widely used approach is to detect f_{CEO} at the oscillator output and modulate the pump laser intensity to stabilize it [10]. Another technique denoted as feed-forward stabilization [6] consists in using the -1 diffraction order of an Acousto-Optic Frequency Shifter (AOFS) driven at the measured f_{CEO} at the oscillator cavity output. Using this technique, CEP fluctuations lower than 30 mrad over 24 hours have been reported by Luecking et al. [11]. Long-term CEP stabilization is, however, difficult using only the feed-forward approach, because of f_{CEO} drifting out of the AOFS bandwidth. Recently, a hybrid approach combining the feed-forward technique and a slow feedback loop has been proposed to overcome this limitation [12].

Active CEP-stable amplified setups are realized starting with a CEP-stable oscillator and using a feedback loop to correct the CEP fluctuations acquired along the amplification chain. The CEP fluctuations are measured at the laser system output and corrected using a CEP actuator. For example, an electro-optic modulator can be used [13,14]. The complexity and cost of an all active stabilization approach is a main drawback for these CEP-stable systems.

On the other hand, passive CEP stabilization is an all-optical approach based on the difference frequency generation (DFG) [15,16] process. The f_{CEO} is set to zero by performing DFG between two pulses carrying the same CEP. The main advantage in this case is to avoid any feedback and locking electronics, simplifying the setup and reducing system costs. For oscillators, a non CEP-stable oscillator is spectrally broadened in a photonic crystal fiber to produce an octave spanning spectrum and DFG is performed between two parts of the spectrum to obtain a CEP-stable signal [17]. Passive stabilization can also be applied to amplified pulses, in Optical Parametric Amplifier (OPA) and Optical Parametric Chirped Pulse Amplifier (OPCPA) architectures. Also in these cases, the oscillator is not required to be CEP-stable [18,19]. The DFG can be realized in the last OPA stage [20] or at an intermediate amplification stage and the CEP-stable signal is amplified through successive stages [21]. For reliable CEP-stable sources, an active stabilization loop must be added even in passive stabilization architectures to ensure an application-ready setup. Indeed, CEP-stable OP(CP)A systems often require an active slow-loop CEP correction for compensating the interferometric (thermal, acoustic) drifts of the setup. As the power and energy of these sources is continuously increasing [22–25], the impact of these fluctuations tends to increase as well. To this end, another active element is usually inserted in the laser chain to act on the CEP in the slow-loop. For instance, an Acousto-Optic Programmable Dispersive Filter (AOPDF, Dazzler, Fastlite) is used by Budriunas et al. [21] for this purpose but comes at the expense of increased system complexity and additional losses.

Moreover, it is commonly required for the applications to change and modulate the CEP. For all-actively stabilized setups, this is obtained by using the stabilization electronics. In passively stabilized systems, a new element must be added for this purpose, such as a motorized pair of wedges [26]. The added active element must be carefully chosen given the required bandwidth of the CEP modulation.

In this article, we present a simple way to control the CEP in passively stabilized sources. The technique exploits the white light generation (WLG) process, already present in DFG schemes, and only requires to modulate the pump laser intensity, which is a possibility often included in commercial laser sources. We describe the concept and demonstrate it experimentally. We first use it to control and modulate the CEP at the system output. In a second step, the technique is used in a feedback loop to correct slow CEP fluctuations in an OPA. The proposed actuator results in a lossless, simple active element to be used for CEP slow-loop feedback drift compensation in OPA/OPCPA setups.

2. Principle

The principle of the proposed CEP actuator relies on the amplitude to phase coupling occurring in the WLG process. This phenomenon has been studied in details by Baltuska et al. [27]. It is possible to find a WLG condition such that the pump laser intensity modulation is linearly transferred to phase on the WLG output. The WLG process is used in the OPA/DFG based passive CEP stabilization to generate the signal. Let us consider the principle depicted in Fig. 1. If two pulses originating from the same pulse train are used in a DFG process, it results in an inherently stable CEP output because the phase terms φ_{CEP} cancel out. In a more realistic model, the WLG process, as well as all differential phases accumulated between the separation of both pulses and the DFG, have to be included. As shown in Fig. 1, modifying the WLG-induced phase results in a signal carrying a new phase term $\varphi_{\text{CEP,WLG}}$.

If the pump laser intensity is modulated, the DFG output is modulated in CEP because of the WLG dependent added phase term. Let us, for example, consider a sinusoidal modulation with amplitude $\sigma_1/2$, as shown in Fig. 2. The DFG output is modulated sinusoidally in CEP with an amplitude of $\alpha * \sigma_1$. The parameter α is dependent on the WLG conditions. Carefully choosing the WLG conditions, a CEP modulation over 2π at the DFG output is obtained with a pump intensity variation of a few percent. The DFG output can be highly modulated in CEP while

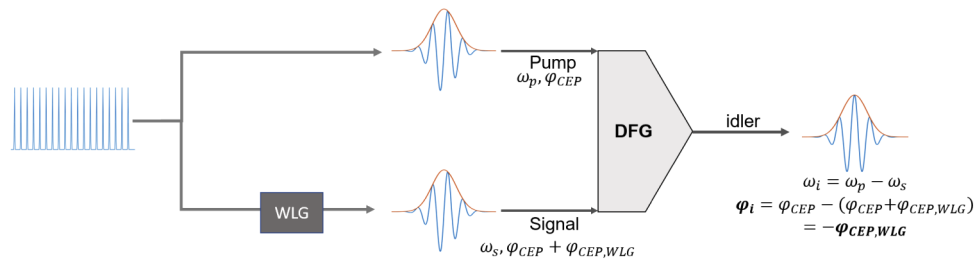


Fig. 1. CEP actuator principle. DFG scheme where a WLG process is involved for the signal generation.

maintaining small enough intensity fluctuations for the system application. Moreover, the output intensity fluctuations are often further reduced in the case of subsequent saturated amplification or nonlinear conversion stages [28]. For instance, this applies when the DFG is the first of several amplification stages in an OPCPA source.

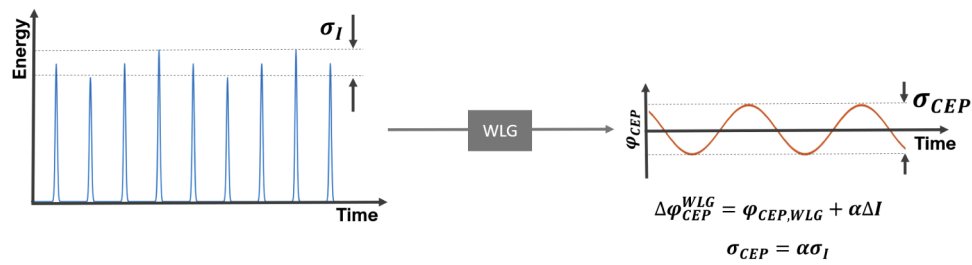


Fig. 2. Principle scheme for the intensity to CEP modulation coupling in the WLG process.

3. Experimental setup

The experimental setup is depicted in Fig. 3, and is similar to part of the system described in [14]. It is a passively CEP-stable high repetition rate laser system including the proposed actuator. It starts with a commercial Yb-doped laser delivering 40 μ J, 300 fs pulses at 100 kHz (Satsuma, Amplitude), with a typical relative intensity noise of 0.5%. This laser source is used to pump a white light-seeded OPA. The laser is frequency doubled to obtain a 515 nm central wavelength. A fraction of the energy is used to generate a signal centered at 690 nm via the WLG process. The OPA output idler is emitted at 2060 nm and is inherently CEP-stable. It is frequency-doubled in order to obtain a CEP-stable signal centered at 1030 nm. This choice is due to an easier availability of characterization tools at 1030 nm with respect to 2060 nm. The CEP stability measurement is realized using an inline f-2f interferometer [29]. The f-2f is composed of a 3 mm-thick YAG crystal to generate the octave spanning spectrum and a 1 mm-thick BBO for frequency-doubling. A polarizer cube is used to maximize the fringe contrast, projecting the two interfering beams on the same polarization axis. The obtained CEP-dependent fringes are detected at the output of the f-2f interferometer using a commercial fast CEP detector (Fringeazz, Fastlite) allowing to measure single shot CEP values at 100 kHz repetition rate with 10 kHz maximum sampling rate. A spectrometer is used as an alternative method for measuring the CEP. The CEP actuator is first characterized in terms of its ability to modulate the CEP. The pump intensity modulation is obtained by operating on the transmittance of an Acousto-Optic Modulator (AOM) included at the output of the pump laser, before the compressor unit. This element is standard in most of commercially available industrial-grade pump laser. A waveform

generator is used to apply different signals to the AOM, and assess how this is translated to the output CEP. In a second step this method is used in a CEP feedback loop using the Fringezzz obtained error signal, and a commercial PID unit connected to the AOM transmittance efficiency.

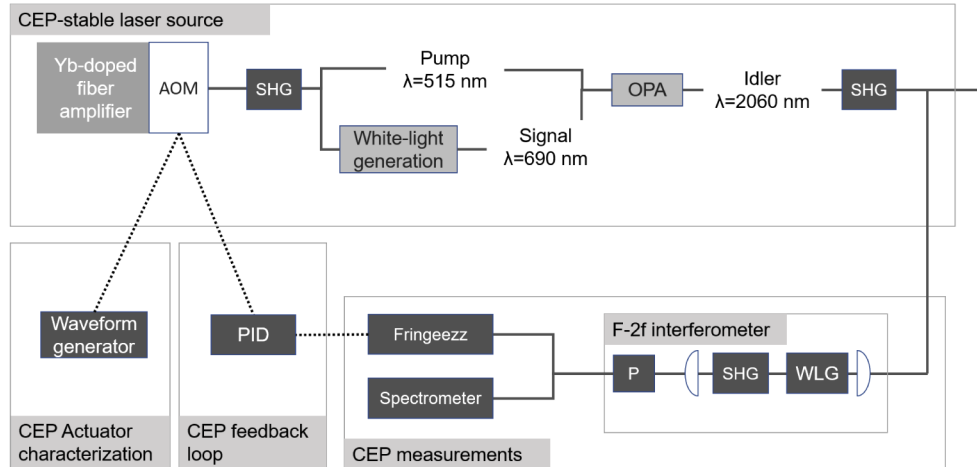


Fig. 3. Experimental setup. AOM= Acousto-Optic Modulator; SHG=Second Harmonic Generation; WLG= White-Light Generation; P=Polarizer cube; PID= Proportional-Integrative-Derivative controller.

4. Optimal WLG operating point

The crucial point of the proposed approach is to operate the WLG in conditions that result in a linear transfer between the pump laser intensity and the output CEP. This condition is met when a stable filament is obtained in the crystal used for the WLG. Studying the amplitude noise [30] transfer through the WLG process allows to determine unambiguously the stable filament condition. For this scope, the RMS pulse-to-pulse stability of the WLG signal is measured using a 10 nm bandpass filter centered at 690 nm, a fast photodiode and an oscilloscope. 10,000 pulses are acquired for each stability measurement. The pulse-to-pulse stability with respect to the energy used for the WLG is reported in blue in Fig. 4. No modulation is applied on the AOM at the pump laser output. The measured pulse stability at the WLG output depends only on the pump laser amplitude noise and on the WLG conditions. For energies ranging between 520 nJ and 560 nJ, the measured pulse-to-pulse variation is minimum with a stability of 1.2% rms. This range corresponds to the stable filament condition. The DFG output pulse-to-pulse stability is measured and plotted in red in Fig. 4 to complete the system analysis. For the DFG output, the best stability conditions are found between 525 nJ and 550 nJ WLG input energy, with a recorded stability of 0.5% rms. Both WLG signal and DFG output must have the highest pulse-to-pulse stability for optimum CEP actuator operation. The grey-shaded area in Fig. 4 outlines the optimal operating zone, ensuring linearity of the amplitude to phase coupling in the WLG process and to the DFG output [27].

The CEP at the output of the system is measured using an f-2f interferometer, that also involves a WLG process. Intensity-to-phase coupling is unavoidable in the f-2f WLG process, so that input intensity fluctuations are coupled to the measured CEP values [31]. The measured CEP value in the free-running case is therefore both affected by the “true” CEP resulting from intensity-to-phase coupling in the DFG stage and by intensity-to-phase coupling in the f-2f interferometer. In the presented setup, the DFG process is saturated, so that the intensity variations of the CEP-stable idler are reduced by 40% with respect to the pump laser. The intensity-to-phase

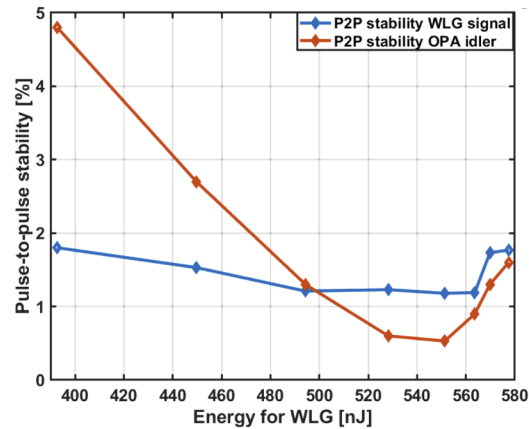


Fig. 4. Pulse-to-pulse stability with respect to the WLG input energy. (Blue) WLG pulse-to-pulse stability, (red) DFG output pulse-to-pulse stability.

coupling induced by the WLG process in the f - $2f$ interferometer is therefore lower than the one observed in the DFG stage WLG. More generally, high energy CEP-stable systems will necessarily require the implementation of further amplification stages, which leads to stronger saturation and further reduced intensity fluctuations. This will decrease the impact of intensity fluctuations induced by the actuator on the CEP value measured by the f - $2f$ device. Ultimately, the specific intensity-to-phase coupling coefficient of the implemented f - $2f$ interferometer could be calibrated and subtracted from the f - $2f$ measured value by performing simultaneous energy measurement, as suggested in [32,33]. This coupling coefficient depends on the specific parameters of the WLG and the f - $2f$ interferometer, such as the focusing conditions inside the WLG material.

5. Results

5.1. CEP actuator

The CEP actuator is characterized by measuring the CEP at the output of the passively stabilized system. We apply a modulation on the AOM transmission efficiency. Three different signals are applied. First, we use a sine wave at 50 Hz with an amplitude corresponding to 1.2% peak-to-peak of the laser power. Second, we apply a sinusoidal signal at 25 Hz with an amplitude corresponding to 4.6% peak-to-peak of the laser power. Third, we apply a triangle-shaped signal with the same frequency and amplitude as in the first case. We measure the CEP values at the output of the passively stabilized system. We use the spectrometer with an integration time of 1 ms and a sampling rate of 3 ms over a 0.15 s measurement time. In Fig. 5 (left) the measured fringe patterns for the three cases are reported. It is clear that the applied pump laser intensity modulations are measured as CEP modulations on the passively-stabilized output. In Fig. 5 (right) the CEP variations are retrieved using a Fourier Transform Spectral Interferometer (FTSI) algorithm [34]. In case (a) of Fig. 5, the relative power to CEP transfer coefficient has a value of 1.3 rad/% corresponding to a CEP modulation amplitude of 1.6 rad peak-to-peak. The linearity of the CEP actuator is tested in case (b). The applied sinusoidal signal has a peak-to-peak amplitude about 4 times that of case (a). The measured CEP amplitude is 6 rad peak-to-peak, which confirms the linearity of the transfer. The actuator operation bandwidth is also characterized applying a sinusoidal waveform at different frequencies spanning from 1 Hz up to 10 kHz. Linear and constant transfer of the pump laser intensity modulation to the CEP output is measured for all applied frequencies.

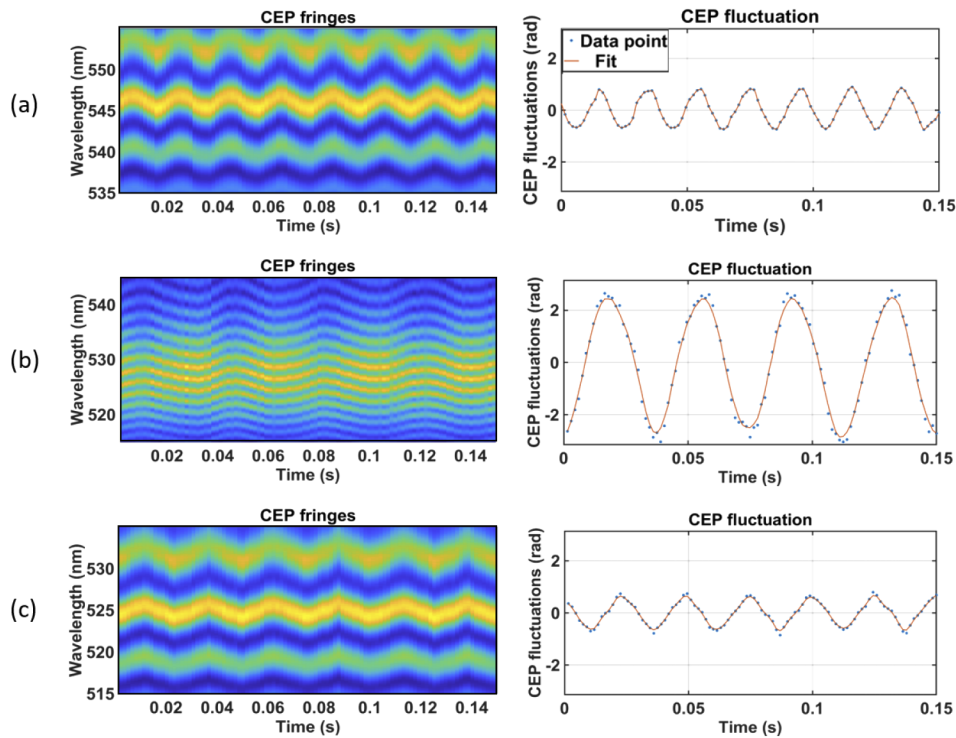


Fig. 5. Left: spectrometer acquired fringe patterns over 0.15s. Right: Extracted CEP as a function of time via a FTSI algorithm.

5.2. CEP feedback loop

The CEP actuator is now tested in a feedback loop scheme to correct the slow CEP fluctuations at the output of the passively stabilized system. The feedback loop is composed of the CEP detection (f-2f and Fringezzz), a commercial PID unit, and the proposed actuator. The detector integration time is 10 μ s, at a sampling rate of 10 kHz.

In Fig. 6(a), the measured CEP is displayed over 7.4 s, with the feedback loop being tuned on at 4.3 s. In Fig. 6(b)(top) the CEP noise power spectral density is plotted over [0.1 Hz; 5 kHz] for the feedback off case (blue line) and the feedback on case (red line). The integrated CEP noise is shown on the bottom of Fig. 6(b). The integrated CEP noise over the measured bandwidth is reduced from 900 mrad to 300 mrad when the feedback loop is activated. The CEP noise in the low frequency range is efficiently suppressed by the feedback. The correction bandwidth is limited to 5 kHz by the detector sampling rate and can be improved using a faster detector.

The long-term action of the feedback loop is measured to complete the system analysis. In Fig. 7, the CEP fluctuations over more than 50 minutes are reported. The measured CEP noise is 380 mrad. This result confirms the reliability of the method on the long-term time scale.

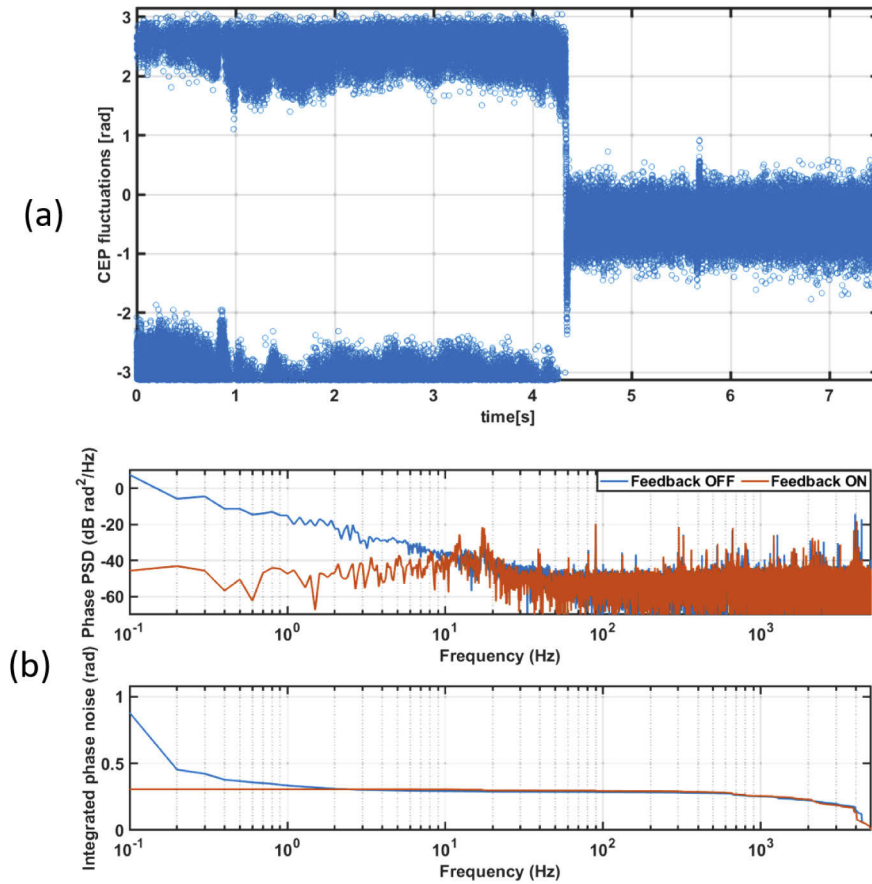


Fig. 6. (a) CEP fluctuations measurement without and with feedback loop. (b) (Top) Power Spectral Density (PSD) and (Bottom) integrated phase noise for CEP fluctuations with feedback loop on (red plot) and off (blue).

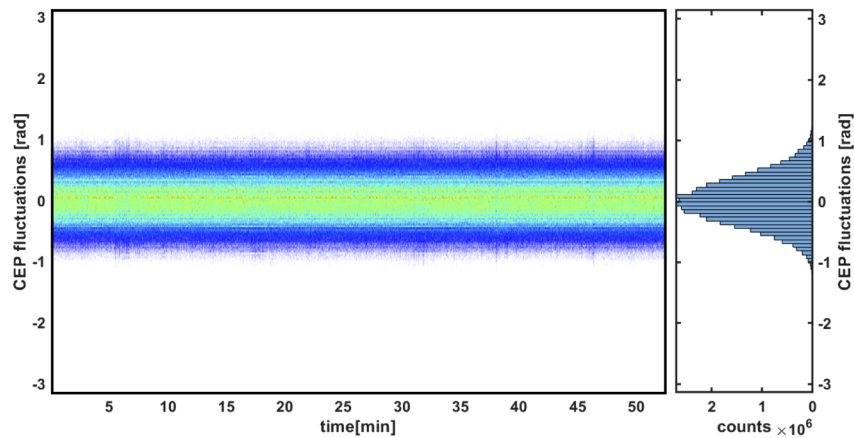


Fig. 7. CEP fluctuations measurement over 52 minutes.

6. Conclusions

We propose a CEP actuator for passively stabilized source architectures. It is based on the use of the WLГ process and the associated amplitude to phase coupling. Modulating the pump laser intensity allows to act on the CEP. A method to optimize the operation conditions of the WLГ, required to implement the method efficiently, is reported. An experimental demonstration of the idea is realized using an AOM at the output of the Yb-doped fiber amplifier that pumps a DFG-based CEP-stable source. The actuator is characterized by modulating the pump laser intensity with different waveforms, showing the linearity of the amplitude to CEP transfer. The CEP actuator is then used in a feedback loop to correct fluctuations of the passive CEP stabilization scheme. The results show efficient attenuation of the CEP noise up to 5 kHz, limited by the detection sampling rate. The proposed CEP actuator relies on a very simple and easily applicable concept. It can be used for a large number of purposes. The modulation of the WLГ pump laser intensity can be realized using different active elements such as a Pockels cell or a liquid crystal modulator instead of the AOM. We believe that the demonstrated scheme is a perfect fit for amplified passively-stabilized sources such as high energy and high power OPCPA CEP-stable laser systems.

Funding. Agence Nationale de la Recherche (ANR-16-CE30-0027-01).

Disclosures. The authors declare no conflicts of interest.

Data availability. Data underlying the results presented in this paper are not publicly available at this time but may be obtained from the authors upon reasonable request.

References

1. J. Kim and Y. Song, "Ultralow-noise mode-locked fiber lasers and frequency combs: principles, status, and applications," *Adv. Opt. Photonics* **8**(3), 465–540 (2016).
2. A. S. Kowligy, H. Timmers, A. J. Lind, U. Elu, F. C. Cruz, P. G. Schunemann, J. Biegert, and S. A. Diddams, "Infrared electric field sampled frequency comb spectroscopy," *Sci. Adv.* **5**(6), eaaw8794 (2019).
3. B. Wolter, M. G. Pullen, M. Baudisch, M. Sclafani, M. Hemmer, A. Senfleben, C. D. Schröter, J. Ullrich, R. Moshhammer, and J. Biegert, "Strong-field physics with mid-IR fields," *Phys. Rev. X* **5**(2), 021034 (2015).
4. P. Rác, S. Irvine, M. Lenner, A. Mitrofanov, A. Baltuška, A. Elezzabi, and P. Dombi, "Strong-field plasmonic electron acceleration with few-cycle, phase-stabilized laser pulses," *Appl. Phys. Lett.* **98**(11), 111116 (2011).
5. G. Sansone, E. Benedetti, F. Calegari, C. Vozzi, L. Avaldi, R. Flammini, L. Poletto, P. Villoresi, C. Altucci, R. Velotta, S. Stagira, S. De Silvestri, and M. Nisoli, "Isolated single-cycle attosecond pulses," *Science* **314**(5798), 443–446 (2006).
6. S. Koke, C. Grebing, H. Frei, A. Anderson, A. Assion, and G. Steinmeyer, "Direct frequency comb synthesis with arbitrary offset and shot-noise-limited phase noise," *Nat. Photonics* **4**(7), 462–465 (2010).
7. B. Borchers, S. Koke, A. Husakou, J. Herrmann, and G. Steinmeyer, "Carrier-envelope phase stabilization with sub-10 as residual timing jitter," *Opt. Lett.* **36**(21), 4146–4148 (2011).
8. A. Golinelli, X. Chen, E. Gontier, B. Bussièrre, O. Tcherbakoff, M. Natile, P. d'Oliveira, P.-M. Paul, and J.-F. Hergott, "Original Ti: Sa 10 kHz front-end design delivering 17 fs, 170 mrad CEP stabilized pulses up to 5 W," *Opt. Lett.* **42**(12), 2326–2329 (2017).
9. D. J. Jones, S. A. Diddams, J. K. Ranka, A. Stentz, R. S. Windeler, J. L. Hall, and S. T. Cundiff, "Carrier-envelope phase control of femtosecond mode-locked lasers and direct optical frequency synthesis," *Science* **288**(5466), 635–639 (2000).
10. A. Poppe, R. Holzwarth, A. Apolonski, G. Tempea, C. Spielmann, T. W. Hänsch, and F. Krausz, "Few-cycle optical waveform synthesis," *Appl. Phys. B* **72**(3), 373–376 (2001).
11. F. Lücking, A. Assion, A. Apolonski, F. Krausz, and G. Steinmeyer, "Long-term carrier-envelope-phase-stable few-cycle pulses by use of the feed-forward method," *Opt. Lett.* **37**(11), 2076–2078 (2012).
12. J. Hirschman, R. Lemons, E. Chansky, G. Steinmeyer, and S. Carbajo, "Long-term hybrid stabilization of the carrier-envelope phase," *Opt. Express* **28**(23), 34093–34103 (2020).
13. J.-F. Hergott, O. Tcherbakoff, P.-M. Paul, P. Demengeot, M. Perdrix, F. Lepetit, D. Garzella, D. Guillaumet, M. Comte, P. D'Oliveira, and O. Gobert, "Carrier-Envelope Phase stabilization of a 20 W, grating based, chirped-pulse amplified laser, using Electro-Optic effect in a LiNbO₃ crystal," *Opt. Express* **19**(21), 19935–19941 (2011).
14. M. Natile, A. Golinelli, L. Lavenue, F. Guichard, M. Hanna, Y. Zaouter, R. Chiche, X. Chen, J. Hergott, W. Boutu, H. Merdji, and P. Georges, "CEP-stable high-energy ytterbium-doped fiber amplifier," *Opt. Lett.* **44**(16), 3909–3912 (2019).
15. C. Manzoni, G. Cerullo, and S. De Silvestri, "Ultrabroadband self-phase-stabilized pulses by difference-frequency generation," *Opt. Lett.* **29**(22), 2668–2670 (2004).

16. M. Zimmermann, C. Gohle, R. Holzwarth, T. Udem, and T. W. Hänsch, "Optical clockwork with an offset-free difference-frequency comb: accuracy of sum-and difference-frequency generation," *Opt. Lett.* **29**(3), 310–312 (2004).
17. T. Hellerer, "Laser device for production of a frequency comb free of CEO," (2014). US Patent 8, 811, 435.
18. G. Cerullo, A. Baltuška, O. D. Muecke, and C. Vozzi, "Few-optical-cycle light pulses with passive carrier-envelope phase stabilization," *Laser Photonics Rev.* **5**(3), 323–351 (2011).
19. N. Thiré, R. Maksimenka, B. Kiss, C. Ferchaud, G. Gitzinger, T. Pinoteau, H. Jousset, S. Jarosch, P. Bizouard, V. Di Pietro, E. Cormier, K. Osvay, and N. Forget, "Highly stable, 15 W, few-cycle, 65 mrad CEP-noise mid-IR OPCPA for statistical physics," *Opt. Express* **26**(21), 26907–26915 (2018).
20. H. Çankaya, A.-L. Calendron, C. Zhou, S.-H. Chia, O. D. Mücke, G. Cirmi, and F. X. Kärtner, "40- μ J passively CEP-stable seed source for ytterbium-based high-energy optical waveform synthesizers," *Opt. Express* **24**(22), 25169–25180 (2016).
21. R. Budriūnas, T. Stanislauskas, and A. Varanavičius, "Passively CEP-stabilized frontend for few cycle terawatt OPCPA system," *J. Opt.* **17**(9), 094008 (2015).
22. M. K. Windeler, K. Mecseki, A. Miahnahri, J. S. Robinson, J. M. Fraser, A. R. Fry, and F. Tavella, "100 W high-repetition-rate near-infrared optical parametric chirped pulse amplifier," *Opt. Lett.* **44**(17), 4287–4290 (2019).
23. K. Mecseki, M. K. Windeler, A. Miahnahri, J. S. Robinson, J. M. Fraser, A. R. Fry, and F. Tavella, "High average power 88 W OPCPA system for high-repetition-rate experiments at the LCLS x-ray free-electron laser," *Opt. Lett.* **44**(5), 1257–1260 (2019).
24. R. Riedel, M. Schulz, M. Prandolini, A. Hage, H. Höppner, T. Gottschall, J. Limpert, M. Drescher, and F. Tavella, "Long-term stabilization of high power optical parametric chirped-pulse amplifiers," *Opt. Express* **21**(23), 28987–28999 (2013).
25. S. Prinz, M. Häfner, M. Schultze, C. Y. Teisset, R. Bessing, K. Michel, R. Kienberger, and T. Metzger, "Active pump-seed-pulse synchronization for OPCPA with sub-2-fs residual timing jitter," *Opt. Express* **22**(25), 31050–31056 (2014).
26. J. Rothardt, S. Demmler, S. Hädrich, J. Limpert, and A. Tünnermann, "Octave-spanning OPCPA system delivering CEP-stable few-cycle pulses and 22 W of average power at 1 MHz repetition rate," *Opt. Express* **20**(10), 10870–10878 (2012).
27. A. Baltuska, M. Uiberacker, E. Goulielmakis, R. Kienberger, V. S. Yakovlev, T. Udem, T. W. Hänsch, and F. Krausz, "Phase-controlled amplification of few-cycle laser pulses," *IEEE J. Sel. Top. Quantum Electron.* **9**(4), 972–989 (2003).
28. P. Hamm, R. A. Kaindl, and J. Stenger, "Noise suppression in femtosecond mid-infrared light sources," *Opt. Lett.* **25**(24), 1798–1800 (2000).
29. M. Kakehata, H. Takada, Y. Kobayashi, K. Torizuka, Y. Fujihira, T. Homma, and H. Takahashi, "Single-shot measurement of carrier-envelope phase changes by spectral interferometry," *Opt. Lett.* **26**(18), 1436–1438 (2001).
30. R. P. Scott, C. Langrock, and B. H. Kolner, "High-dynamic-range laser amplitude and phase noise measurement techniques," *IEEE J. Sel. Top. Quantum Electron.* **7**(4), 641–655 (2001).
31. C. Li, E. Moon, H. Mashiko, H. Wang, C. M. Nakamura, J. Tackett, and Z. Chang, "Mechanism of phase-energy coupling in f-to-2f interferometry," *Appl. Opt.* **48**(7), 1303–1307 (2009).
32. C. Li, E. Moon, H. Wang, H. Mashiko, C. M. Nakamura, J. Tackett, and Z. Chang, "Determining the phase-energy coupling coefficient in carrier-envelope phase measurements," *Opt. Lett.* **32**(7), 796–798 (2007).
33. C. Marceau, G. Gingras, S. Thomas, Y. Kassimi, and B. Witzel, "Energy-phase coupling inside sapphire-based f-2f nonlinear interferometers from 800 to 1940 nm," *Appl. Opt.* **53**(5), 898–901 (2014).
34. M. Takeda, H. Ina, and S. Kobayashi, "Fourier-transform method of fringe-pattern analysis for computer-based topography and interferometry," *J. Opt. Soc. Am.* **72**(1), 156–160 (1982).